AIP | Applied Physics Letters

Comparison of the growth kinetics of In2O3 and Ga2O3 and their suboxide desorption during plasma-assisted molecular beam epitaxy

Patrick Vogt and Oliver Bierwagen

Citation: Applied Physics Letters **109**, 062103 (2016); doi: 10.1063/1.4960633
View online: http://dx.doi.org/10.1063/1.4960633
View Table of Contents: http://scitation.aip.org/content/aip/journal/apl/109/6?ver=pdfcov
Published by the AIP Publishing

Articles you may be interested in

Reaction kinetics and growth window for plasma-assisted molecular beam epitaxy of Ga2O3: Incorporation of Ga vs. Ga2O desorption
Appl. Phys. Lett. **108**, 072101 (2016); 10.1063/1.4942002

Growth model for plasma-assisted molecular beam epitaxy of N-polar and Ga-polar In x Ga 1 − x N
J. Vac. Sci. Technol. B **29**, 021206 (2011); 10.1116/1.3562277

Rf-plasma-assisted molecular-beam epitaxy of β - Ga 2 O 3
Appl. Phys. Lett. **88**, 031105 (2006); 10.1063/1.2164407

Growth kinetics of AlGaN films by plasma-assisted molecular-beam epitaxy
Appl. Phys. Lett. **81**, 295 (2002); 10.1063/1.1492853

Kinetic modeling of N incorporation in GaInNAs growth by plasma-assisted molecular-beam epitaxy
Appl. Phys. Lett. **77**, 214 (2000); 10.1063/1.126928

Reuse of AIP Publishing content is subject to the terms at: https://publishing.aip.org/authors/rights-and-permissions. Download to IP: 62.141.165.1 On: Mon, 08 Aug 2016 14:32:49

Comparison of the growth kinetics of In_2O_3 and Ga_2O_3 and their suboxide desorption during plasma-assisted molecular beam epitaxy

Patrick Vogt[a] and Oliver Bierwagen[b]
Paul-Drude-Institut für Festkörperelektronik, Hausvogteiplatz 5–7, D-10117 Berlin, Germany

(Received 14 June 2016; accepted 25 July 2016; published online 8 August 2016)

We present a comprehensive study of the In_2O_3 growth kinetics during plasma-assisted molecular beam epitaxy and compare it to that of the related oxide Ga_2O_3 [P. Vogt and O. Bierwagen, Appl. Phys. Lett. **108**, 072101 (2016)]. The growth rate and desorbing fluxes were measured during growth *in-situ* by a laser reflectometry set-up and line-of-sight quadrupole mass spectrometer, respectively. We extracted the In incorporation as a function of the provided In flux, different growth temperatures T_G, and In-to-O flux ratios r. The data are discussed in terms of the competing formation of In_2O_3 and desorption of the suboxide In_2O and O. The same three growth regimes as in the case of Ga_2O_3 can be distinguished: (i) In-transport limited, O-rich (ii) In_2O-desorption limited, O-rich, and (iii) O-transport limited, In-rich. In regime (iii), In droplets are formed on the growth surface at low T_G. The growth kinetics follows qualitatively that of Ga_2O_3 in agreement with their common oxide and suboxide stoichiometry. The quantitative differences are mainly rationalized by the difference in In_2O and Ga_2O desorption rates and vapor pressures. For the In_2O, Ga_2O, and O desorption, we extracted the activation energies and frequency factors by means of Arrhenius-plots. *Published by AIP Publishing*. [http://dx.doi.org/10.1063/1.4960633]

The transparent (semi)conducting oxide indium sesquioxide, In_2O_3, possesses a wide range of conventional device applications based on its conductivity and large band gap of $E_g = (2.7 \pm 0.1)$ eV.[1] Undoped In_2O_3 is used as an active gas-sensor material,[2,3] for instance. In_2O_3 highly doped with tin, indium-tin oxide (ITO, In_2O_3:Sn), is a transparent conducting oxide that is used as a transparent contact electrode for flat panel displays[4] or solar cells.[5]

Beyond these conventional applications, In_2O_3 has the potential for novel applications[1] that benefit from well defined doping, e.g., with the donor Sn or the (deep) acceptor Mg, controlling the *n*-type conductivity from the highly conductive[6] to the semi-insulating[7] regime. In combination with the related gallium sesquioxide, Ga_2O_3, with $E_g = (4.7 \pm 0.2)$ eV,[8] band gap engineering and heterostructure oxide devices are foreseeable.[9] The realization of semiconductor devices typically requires the highest crystalline quality which is commonly achieved by epitaxial growth methods. During plasma-assisted molecular beam epitaxy (MBE), fluxes of atomic In Φ_{In} and plasma "activated" oxygen Φ_O form In_2O_3 on a heated, single crystalline substrate in an ultra-high vacuum chamber. MBE-grown In_2O_3 has been reported on $Al_2O_3(0001)$,[3,10,11] $(10\bar{1}2)$[12] $(11\bar{2}0)$,[13] and Y-stabilized $ZrO_2(001)$[14] or (111),[3] for instance.

Oxides are typically grown under O-rich growth conditions, i.e., by providing excess O for the reaction with In. However, the In-rich growth conditions are known to improve the structural quality of $In_2O_3(001)$[15,16] by preventing faceting and should also help to suppress the formation of compensating acceptor point defects (oxygen interstitials or metal vacancies).[17]

The growth rate Γ of In_2O_3 is limited by Φ_{In} under O-rich growth conditions, and thus increases linearly with it up to the stoichiometric flux Φ_{SF} which consumes all available oxygen for the In_2O_3 formation.[18] At $\Phi_{In} > \Phi_{SF}$, the In-rich growth regime is entered, where Γ decreases with increasing Φ_{In} due to the oxygen-deficiency-induced formation of the volatile suboxide In_2O, which desorbs off subsequently.[18]

We have shown qualitatively the same behavior for the related oxide Ga_2O_3 which has the same oxide and suboxide stoichiometry.[18,19] Furthermore, our comprehensive investigation of Ga_2O_3 growth revealed a Γ-plateau in the O-rich regime at high growth temperatures T_G, which was also due to the suboxide desorption of Ga_2O.

In this letter, we show how Γ is governed by the competition between In_2O_3 layer growth and desorption of In_2O and O as a function of T_G, Φ_{In}, and Φ_O. We use the same methodology as for Ga_2O_3[19] and show that the reaction kinetics of In_2O_3 and Ga_2O_3 have qualitatively the same behaviour. The quantitative differences of the Γ-evolutions of In_2O_3 and Ga_2O_3 are analyzed by fitting the desorbing In_2O, Ga_2O, and O fluxes as a function T_G on an Arrhenius-plot and extract the activation energies $E^i_{a,des}$ as well as the frequency factors A_i of both materials. Finally, we rationalize these differences by the different In_2O and Ga_2O desorption activation energies and their vapor pressures.

Textured, non-polycrystalline $In_2O_3(111)$ with rotational domains[3,11] was grown on single-side polished 2 inch $Al_2O_3(0001)$ substrates. The rough back side of the substrate was sputter-coated with titanium to improve substrate heating. During growth, T_G was measured with a pyrometer. A low T_G nucleation layer was used to ensure complete wetting[14] of the substrate and mimic homoepitaxy. Our custom made MBE system is equipped with a laser reflectometry set-up and line-of-sight quadrupole mass spectrometer (QMS) that allow to measure *in-situ* Γ and the desorbing In_2O from the In_2O_3 growth surface $\Phi^{In_2O}_{des}$, respectively.[18,19]

[a]Electronic mail: vogt@pdi-berlin.de
[b]Electronic mail: bierwagen@pdi-berlin.de

Reuse of AIP Publishing content is subject to the terms at: https://publishing.aip.org/authors/rights-and-permissions. Download to IP: 62.141.165.1 On: Mon, 08 Aug 2016 14:32:49

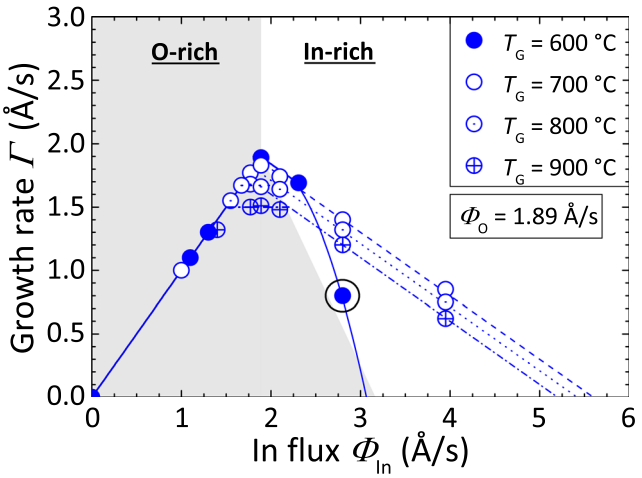

FIG. 1. The In_2O_3 growth rate Γ as a function of the In flux Φ_{In} at constant O flux Φ_O of 1.89 Å/s at four different growth temperatures T_G. For $T_G > 700\,°C$, Γ plateaus in the O-rich regime. The lines are guides to the eye.

However, due to the large mass of In_2O of 246 atomic mass units, the signal-to-noise ratio was low, which prevented reliable quantification of $\Phi_{des}^{In_2O}$ by our QMS data. Instead, $\Phi_{des}^{In_2O}$ was determined indirectly as the difference between the provided Φ_{In} and Γ as described below and justified by the same Me-to-O stoichiometry like Ga_2O_3.[19] The crystallinity of the oxide films was verified *in-situ* by a spotty reflection high energy electron diffraction pattern during growth and *ex-situ* by X-ray diffraction ω–2θ scans (not shown). A standard shuttered hot-lip effusion cell was used to evaporate liquid In (7 N purity). The beam equivalent pressure (BEP) which is proportional to the particle flux was measured by a nude filament ion gauge positioned at the substrate location. Following the calibration reported in Refs. 18 and 19, the relation of Φ_{In} between the measured BEP, Γ, and the In-particle flux is $\Phi_{In} = 5.67 \times 10^{-7}$ Torr $\hat{=} 1.0$ Å/s $\hat{=} 3.1$ In-atoms nm^{-2} s^{-1}, respectively. A radio frequency plasma source with a mass flow controller supplied Φ_O from the research-grade O_2 gas (6 N purity). The radio frequency power was maintained at 200 W for the In_2O_3 growth. The O_2 mass flow was set to 0.5 standard cubic centimeters per minute (SCCM) resulting in $\Phi_O = 5 \times 10^{-6}$ Torr $\hat{=}$ 1.89 Å/s $\hat{=}$ 8.85 O-atoms nm^{-2} s^{-1}.

In order to investigate the origin of the In loss during growth and being able to compare it quantitatively with the Ga loss during Ga_2O_3 growth, we conducted the same experiments as reported in Ref. 19.

The Γ-evolution of In_2O_3 as a function of Φ_{In} for different T_G is depicted in Fig. 1. In the O-rich regime and $T_G = 700\,°C$ (open discs), the In incorporation (i.e., Γ) increases linearly with Φ_{In} until the stoichiometric flux ratio is reached at $\Phi_{In} = \Phi_O = 1.89$ Å/s. This ratio corresponds to $r = \Phi_{In}/\Phi_O = 1$. For a higher $r > 1$, the growth shifts into the In-rich regime and Γ decreases until the growth completely stops at $\Phi_{In} \geq 3\Phi_O$[18] showing the same trend in Γ as for Ga_2O_3 growth which is due to the same Me-to-O stoichiometry of these compounds.

In the In-rich regime at lower $T_G = 600\,°C$ (filled discs), In forms droplets on the growth surface as observed by scanning electron microscopy (not shown), which strongly reduces Γ as exemplarily indicated by the black circle in Fig. 1.

Increasing $T_G > 700\,°C$ while keeping Φ_{In} and Φ_O identical leads to a different Γ-evolution. The maximum Γ is decreased in comparison to the growth at $T_G = 700\,°C$. In addition, a plateau of Γ as for the Ga_2O_3 growth[19] in the O-rich regime is present. Comparing the Γ-evolution of In_2O_3 plotted in Fig. 1 with the one of Ga_2O_3 indicates that the loss of Γ is caused by In_2O and O desorption. This behavior is quantitatively described in Ref. 19 for Ga_2O_3 growth and can be readily transferred to the In_2O_3 growth in this letter. The length of the plateau λ is parameterized and defined in Ref. 19 by the fraction of the maximum O flux that is available to oxidize In to In_2O_3 or In_2O, named as α, and the maximum Γ normalized by Φ_O in the O-rich regime, named as β. Note, that the normalization by Φ_O is reasonable since the surface reaction kinetics is determined by the Me-to-O flux ratio as reported in Ref. 19 for Ga_2O_3 and exemplarily shown for In_2O_3 in Fig. 3 different Φ_{In} and Φ_O but same r (filled and crossed discs).

A qualitative explanation that In_2O and not In desorption is responsible for the plateau of Γ in the O-rich regime is the following: the decreasing Γ with increasing r in the In-rich regime for all investigated $T_G > 700\,°C$ is due to the oxygen-deficiency-induced In_2O formation and *not* because of In desorption.[18] For this reason, In desorption instead of In_2O formation and its desorption at even lower r in the O-rich regime (i.e., in the excess of O) is unphysical. Indium desorption, in turn, would lead to a plateau in the In-rich regime (i.e., O-limited growth regime) and not to a decrease of Γ as plotted in Fig. 1.

Three growth regimes of In_2O_3 are the same as in the Ga_2O_3 growth:[19] (i) In-transport-limited O-rich growth regime with full In incorporation (the linear increase of the normalized Γ by Φ_O ($\rho = \Gamma/\Phi_O$) with r), (ii) In_2O-desorption-limited O-rich growth regime with partial In incorporation (the plateau of $\rho = \beta$), and (iii) O-transport-limited In-rich growth regime with partial In incorporation (the decrease of ρ with r).

For regime (i), i.e., for $0 \leq r < \beta \leq 1$, the reaction is

$$r\,2\mathrm{In}(g) + 3\mathrm{O}(g) \rightarrow r\mathrm{In_2O_3}(s) + 3(1-r)\mathrm{O}(g), \quad (1)$$

with g and s indicating the gaseous and solid phases, respectively. The plateau in regime (ii) for $0 < \beta \leq r \leq \beta + \lambda = 3\alpha - 2\beta$ is described by the reaction

$$r\,2\mathrm{In}(g) + 3\mathrm{O}(g) \rightarrow \beta\mathrm{In_2O_3}(s) + (r-\beta)\mathrm{In_2O}(g) + (3 - r + 2\beta)\mathrm{O}(g). \quad (2)$$

The end of the plateau $r = \beta + \lambda$ corresponds to stoichiometric growth conditions. For In-rich growth in regime (iii), $\beta + \lambda < r \leq 3\alpha$, the growth rate decreases and

$$r\,2\mathrm{In}(g) + 3\mathrm{O}(g) \rightarrow \beta\gamma\mathrm{In_2O_3}(g) + (r - \beta\gamma)\mathrm{In_2O}(g) + 3(1-\alpha)\mathrm{O}(g). \quad (3)$$

The coefficient $\gamma = -(r - 3\alpha/2\beta)$ decreases linearly with increasing r from unity at $r = \beta + \lambda = 3\alpha - 2\beta$ to zero at $r = 3\alpha$.

Now we discuss the quantitative differences in the Γ-evolutions of In_2O_3 and Ga_2O_3 regarding the flux range of

Reuse of AIP Publishing content is subject to the terms at: https://publishing.aip.org/authors/rights-and-permissions. Download to IP: 62.141.165.1 On: Mon, 08 Aug 2016 14:32:49

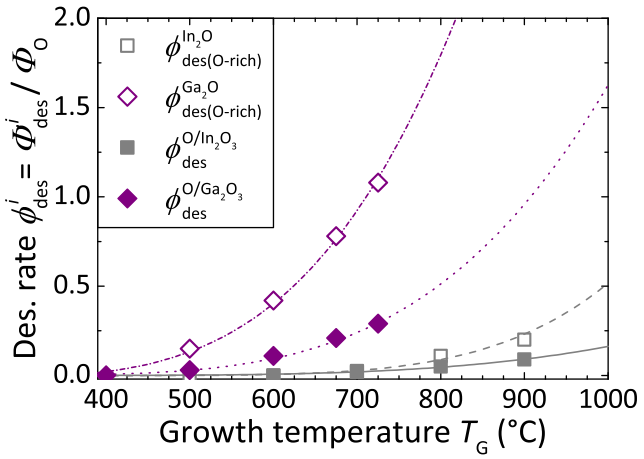

FIG. 2. Maximum desorption rates from the respective growth surface normalized by Φ_O of the suboxides ($\phi^{Me_2O}_{des(O-rich)}$) and O ($\phi^{O/Me_2O_3}_{des}$) as a function of T_G. The lines are Arrhenius-plots according to Eq. (6).

the plateau, the metal adsorption, and suboxide desorption temperature. Figure 2 plots the normalized In_2O (open squares), Ga_2O (open diamonds), and O (filled squares and diamonds) desorption rates from respective In_2O_3 and Ga_2O_3 surfaces $\phi^{Me_2O}_{des(O-rich)}$ and $\phi^{O/Me_2O_3}_{des}$ with Me = In,Ga as a function of T_G. The index (O-rich) refers to the maximum suboxide desorption in the O-rich regime at the end of the plateau where all O is either consumed for layer growth or suboxide formation. The desorption rates are described as

$$\phi^{O/Me_2O_3}_{des}(T_G) = 1 - \alpha(T_G), \tag{4}$$

$$\phi^{Me_2O}_{des(O-rich)}(T_G) = \lambda(T_G) = 3(\alpha(T_G) - \beta(T_G)). \tag{5}$$

In order to obtain the desorption rates in Å/s, these values are multiplied by Φ_O. It can be seen that $\phi^{Ga_2O}_{des(O-rich)} > \phi^{In_2O}_{des(O-rich)}$ and $\phi^{O/Ga_2O_3}_{des} > \phi^{O/In_2O_3}_{des}$ for all measured T_G. The quantitative difference of the Γ-evolutions of In_2O_3 and Ga_2O_3 becomes clear in Fig. 3. Here, for the sake of clarity, Γ is normalized by its maximum value ($\mathcal{R} = \Gamma/\Gamma_{max}$) and plotted as a function of T_G for both materials at different r. For In_2O_3, in the highly O-rich regime (filled and crossed discs) $\mathcal{R}$ is constant over the entire range of T_G. At higher Φ_{In}, for example, at $r = 1$ (stoichiometric growth, open discs) and $r = 1.5$ (In-rich growth, dotted discs) $\mathcal{R}$ decreases slightly due to In_2O and O desorption in both regimes (as also plotted in Figs. 1 and 2). For Ga_2O_3 (triangles), in contrast, the decrease of $\mathcal{R}$ is much stronger due to stronger Ga_2O and O desorption as can be seen by different ϕ^i_{des} with $i = Me_2O$, O/Me_2O_3 for both materials (Fig. 2) that cause the decrease of Γ at the same T_G.

To quantitatively evaluate ϕ^i_{des}, we use exponential fits to the data plotted in Fig. 2

$$\phi^i_{des}(T_G) = A_i \exp\left(-\frac{E^i_{a,des}}{k_B T_G}\right), \tag{6}$$

with k_B the Boltzmann constant. The activation energy of desorption $E^i_{a,des}$ and frequency factor A_i obtained by fitting the data plotted in Fig. 2 by Eq. (6) (Arrhenius-plot) is given in Table I. In Fig. 4, the obtained functions for $\phi^{Me_2O}_{des}$ and

TABLE I. Obtained activation energies for desorption $E^i_{a,des}$ and frequency factors A_i by fitting the data plotted in Fig. 2 by Eq. (6) (Arrhenius-plot).

	In_2O	Ga_2O	O/In_2O_3	O/Ga_2O_3
$E^i_{a,des}$ (eV)	1.03 ± 0.19	0.59 ± 0.01	0.74 ± 0.05	0.68 ± 0.03
$A_i \times 10^3$	6.19	1.04	0.14	0.79

(for comparison to them) the equilibrium vapor pressures p_j with j = In, Ga, In_2O, and Ga_2O as a function of T_G are depicted. We converted the fluxes into units of standard atmospheres (atm) by kinetic theory of gases ($p_k = \Phi^k_{des}\sqrt{2\pi m_k k_B T_G}$ with mass of the suboxide m_k and $k = Ga_2O$, In_2O). It can be seen that the desorbing rates of Ga_2O and In_2O and corresponding vapor pressures show the same trend, i.e., $\phi^{Ga_2O}_{des}$ is larger than $\phi^{In_2O}_{des}$ by roughly one order of magnitude. We conclude that the higher vapor pressure of Ga_2O compared to that of In_2O causes the higher sensitivity of Γ to T_G for Ga_2O_3 growth.

In the In-rich regime (iii) at $T_G \leq 600\,°C$, In forms droplets, whereas no Ga droplet formation was observed under similar growth conditions for Ga_2O_3 growth down to $T_G = 500\,°C$.[19] In order to understand this difference, we quantitatively compare the vapor pressures of the suboxides with the loss of Γ in the Me-rich regime. Exemplarily, we obtain $\phi^{In_2O}_{des} = 4.0 \times 10^{-9}$ atm (star in Fig. 4 and circle in Fig. 1 at $\Phi_{In} = 2.8$ Å/s) and $\phi^{Ga_2O}_{des} = 6.4 \times 10^{-10}$ atm (filled square in Fig. 4 in this letter and Fig. 1 in Ref. 19 at $\Phi_{Ga} = 4$ Å/s) for the loss in Γ of In_2O_3 and Ga_2O_3, respectively. In both cases, p_{In_2O} and p_{Ga_2O} are well in excess of the loss of Γ, which means that In droplet formation is not caused by limited In_2O desorption. As an alternative explanation, we suggest the oxidation velocity of In to In_2O_3 to be slower than that of Ga to Ga_2O_3, since here, all Ga could be oxidized at even lower T_G and p_{Ga_2O}. Comparing p_{In} and p_{Ga} shows that Me desorption for both materials is not the reason for the decreasing Γ in the Me-rich regime.

In summary, we studied the plasma-assisted oxide molecular beam epitaxy of In_2O_3. The In flux, In-to-O flux ratio, and growth temperature were systematically changed

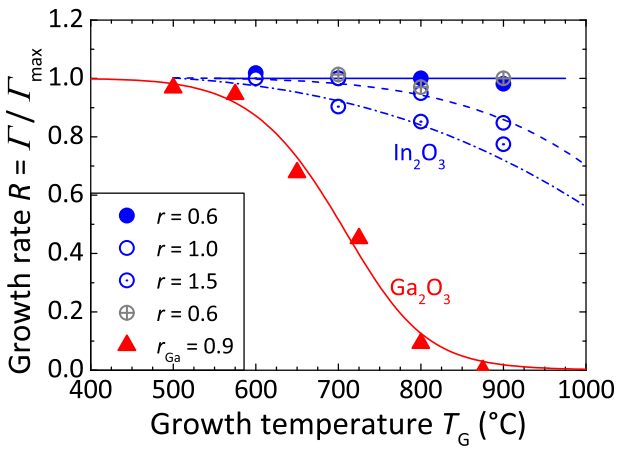

FIG. 3. Growth rate normalized by its maximum value $\mathcal{R} = \Gamma/\Gamma_{max}$ as a function of growth temperature T_G for different In fluxes Φ_{In}. The O flux Φ_O was 1.89 Å/s (filled, open, and dotted discs) and 3.78 Å/s (crossed discs). The triangles show $\mathcal{R}$ for Ga_2O_3 at $r_{Ga} = \Phi_{Ga}/\Phi_O = 0.9$ with $\Phi_O = 1.7$ Å/s. The lines are guides to the eye.

Reuse of AIP Publishing content is subject to the terms at: https://publishing.aip.org/authors/rights-and-permissions. Download to IP: 62.141.165.1 On: Mon, 08 Aug 2016 14:32:49

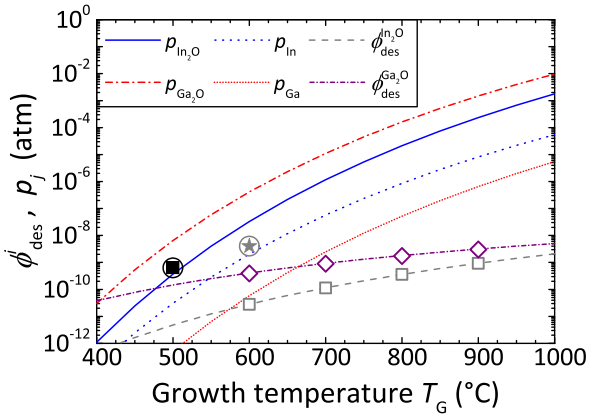

FIG. 4. The normalized desorption rates by Φ_O ($\phi_{des(O-rich)}^{Me_2O}$) and the vapor pressure curves of the suboxides and metals p_j ($j = In_2O$ (solid line[20]), Ga_2O (dashed-dotted line[21]), In (dotted line[22]), Ga (short-dotted red line[22])) as a function of growth temperature T_G are plotted. The lines are functions according to Eq. (6). The filled square and star are quantitative examples of $\phi_{des(O-rich)}^{Ga_2O}$ and $\phi_{des(O-rich)}^{In_2O}$, respectively (values given in the text).

in order to understand the surface reaction kinetics of the In_2O_3 growth and compared it to that of Ga_2O_3 discussed in Ref. 19. In qualitative agreement with Ga_2O_3 growth, our results indicate three distinctive growth regimes: (i) complete In incorporation, i.e., In-transport-limited growth regime (O-rich), (ii) plateau of the growth rate at increasing In flux (In_2O-desorption-limited growth regime, O-rich), and (iii) a decreasing growth rate at increasing In flux, i.e., O-transport-limited growth regime (In-rich). In all cases, the difference between provided fluxes and growth rate is related to the desorption of In_2O and O. No In desorption was observed at all investigated growth temperatures. At lower growth temperatures, in the metal-rich regime, In droplet formation was detected for In_2O_3 whereas for Ga_2O_3 no Ga accumulation was observed under similar growth conditions. As the suboxide vapor pressures cannot explain this qualitative difference, we propose slower oxidation of In than Ga to be the cause. Growth rates lower than the In flux were either caused by the growth in the In rich regime, a higher growth temperature, or In accumulation. The suboxide desorption was fitted by an Arrhenius-plot, yielding activation energies and frequency factors that can be used with Eqs. (4)–(6) to calculate the In_2O_3 and Ga_2O_3 MBE growth rates for all growth temperatures above the metal adsorption temperature. The strong (weak) decrease of the Ga_2O_3 (In_2O_3) growth rate with increasing growth temperature is related to the higher vapor pressure of Ga_2O than that of In_2O.

These findings can be likely transferred to ozone MBE and may also be a qualitative guidance for the In_2O_3 growth by metal-organic chemical vapor deposition. In addition, the overall reaction kinetics might be generalized to all oxides that posses suboxides when knowing their vapor pressures.

We would like to thank Vladimir Kaganer for critically reading the manuscript, Hans-Peter Schönherr for technical MBE support, and Anne-Kathrin Bluhm for SEM imaging.

[1]O. Bierwagen, Semicond. Sci. Technol. **30**, 024001 (2015).
[2]C. Y. Wang, V. Cimalla, T. Kups, C.-C. Röhlig, T. Stauden, O. Ambacher, M. Kunzer, T. Passow, W. Schirmacher, W. Pletschen *et al.*, Appl. Phys. Lett. **91**, 103509 (2007).
[3]J. Rombach, A. Papadogianni, M. Mischo, V. Cimalla, L. Kirste, O. Ambacher, T. Berthold, S. Krischok, M. Himmerlich, S. Selve *et al.*, "The role of surface electron accumulation and bulk doping for gas-sensing explored with single-crystalline In_2O_3 thin films," Sens. Actuators, B (published online).
[4]G. S. Chae, Jpn. J. Appl. Phys., Part 1 **40**, 1282 (2001).
[5]A. N. Tiwari, G. Khrypunov, F. Kurdzesau, D. L. Bätzner, A. Romeo, and H. Zogg, Prog. Photovoltaics: Res. Appl. **12**, 33 (2004).
[6]O. Bierwagen and J. S. Speck, Phys. Status Solidi A **211**, 48 (2014).
[7]O. Bierwagen and J. S. Speck, Appl. Phys. Lett. **101**, 102107 (2012).
[8]M. Higashiwaki, K. Sasaki, H. Murakami, Y. Kumagai, A. Koukitu, A. Kuramata, T. Masui, and S. Yamakoshi, Semicond. Sci. Technol. **31**, 034001 (2016).
[9]S. Fujita and K. Kaneko, J. Cryst. Growth **401**, 588 (2014).
[10]Z. Mei, Y. Wang, X. Du, Z. Zeng, M. Ying, H. Zheng, J. Jia, Q. Xue, and Z. Zhang, J. Cryst. Growth **289**, 686 (2006).
[11]K. H. L. Zhang, V. K. Lazarov, P. L. Galindo, F. E. Oropeza, D. J. Payne, and R. G. Egdell, Cryst. Growth Des. **12**, 1000 (2012).
[12]P. Vogt, A. Trampert, M. Ramsteiner, and O. Bierwagen, Phys. Status Solidi A **212**, 1433 (2015).
[13]M. Y. Chern, Y. C. Huang, and W. L. Xu, Thin Solid Films **515**, 7866 (2007).
[14]O. Bierwagen and J. S. Speck, J. Appl. Phys. **107**, 113519 (2010).
[15]O. Bierwagen, M. E. White, M.-Y. Tsai, and J. S. Speck, Appl. Phys. Lett. **95**, 262105 (2009).
[16]O. Bierwagen, J. Rombach, and J. S. Speck, J. Phys.: Condens. Matter **28**, 224006 (2016).
[17]S. Lany and A. Zunger, Phys. Rev. Lett. **98**, 045501 (2007).
[18]P. Vogt and O. Bierwagen, Appl. Phys. Lett. **106**, 081910 (2015).
[19]P. Vogt and O. Bierwagen, Appl. Phys. Lett. **108**, 072101 (2016).
[20]J. Valderrama-N and K. T. Jacob, Thermochim. Acta **21**, 215 (1977).
[21]C.-J. Frosch and C.-D. Thurmond, J. Phys. Chem. **66**, 877 (1962).
[22]C. B. Alcock, V. P. Itkin, and M. K. Horrigan, Can. Metall. Q. **23**, 309 (1984).

Reuse of AIP Publishing content is subject to the terms at: https://publishing.aip.org/authors/rights-and-permissions. Download to IP: 62.141.165.1 On: Mon, 08 Aug 2016 14:32:49